Real-time Personal Fever Alert Monitoring by Wearable Detector based on Thermoresponsive Hydrogel

Wenbin Wang[1], Chen Wu[2], Kai Zhu[2], Fang Chen[2], Jingjing Zhou[2], Yusuf Shi[1], Chenlin Zhang[1], Renyuan Li[1], Mengchun Wu[1], Sifei Zhuo[2], Hepeng Zhang[2,], Peng Wang[1,3*]*

[1]Water Desalination and Reuse Center, King Abdullah University of Science and Technology, Thuwal 23955-6900, Saudi Arabia.

[2]Key Laboratory of Special Functional and Smart Polymer Materials of Ministry of Industry and Information Technology, School of Chemistry and Chemical Engineering, Northwestern Polytechnical University, Xi'an, 710129, PR China.

[3]Hong Kong Polytechnic University, Hung Hom, Kowloon, Hong Kong, PR China.

*Corresponding author.

E-mail: zhanghepeng@nwpu.edu.cn (H. Zhang), peng.wang@kaust.edu.sa (P. Wang)

KEYWORDS. Fever Screening, body temperature monitoring, thermal sensitive hydrogel, wearable device, PNIPAM, hydrogel.

ABSTRACT. Quick fever screening at mass scale is proven effective during a pandemic to single out the ones with suspected symptoms of infectious diseases. However, achieving affordable and real-time fever alert at individual level, although more preferable, remains elusive. Herein, we report an inexpensive and highly sensitive fever detector which possesses a sharp color-transition temperature window tailor-tuned for fever screening. The sensing component of the detector is rationally designed thermoresponsive agarose@poly(N-isopropylacrylamide)-co-acrylamide (agarose@P(NIPAM-co-AM)) hydrogel. The hydrogel turns from transparent to opaque white, when its temperature is higher than its cloud point. As a proof of concept of its practical applicability, a wearable fever monitoring device was fabricated in the form of a wristband. When the wrist temperature is higher than the threshold of a human fever, the device shows a remarkable color change, alerting an elevated body temperature. The wearable detector provides a promising strategy for real-time fever alert monitoring and is capable of making contributions to inhibit the spread of infectious disease during a pandemic.

Introduction

High body temperature, commonly known as fever, is a defensive body reaction especially to many viral or bacterial infection-related illnesses, such as, severe acute respiratory syndrome (SARS)[1-3], coronavirus disease 2019 (COVID-19)[4-6], influenza[7-9]. When human immune system detects the attack of virus or bacteria, it signals a hypothalamus to turn up the heat to stimulate our immune system. To this end, fever is a typical and early symptom of these infections and thus

monitoring body temperature can help detect these infectious illnesses at an early stage, which is critical for a timely and thus more effective treatment and also helps prevent them from spreading.[10-12]

Body temperature can be taken from many parts of human body, each with its pros and cons[13]. More accurate measures (e.g., taken in mouth, anus, armpit, ear) require direct body contact and are generally accompanied with trivial procedure and lengthy time while fast measures are quick but provide quantitatively less reliable data[14].

During pandemic, mass temperature screening at public places is arguably the most effective way to single out those who have fever and who may have contracted infectious viruses for quarantine and treatment.[15-17] In this case, only fast temperature measures are viable as qualitative determination of whether one's body temperature is above a defined threshold as fever is needed.

During the COVID-19 pandemic, over-head or hand-held infrared thermometers are widely installed or employed to take a person's temperature at entrance of office buildings, campuses, schools, hospitals, supermarkets, airports, and dining halls where people congregate.[18-21] However, these measurements are transient and on a one-off basis. It is known fever symptom associated with virus-led infection develops quickly. Thus, an inexpensive, continuous, and real-time fever alert monitoring, although challenging, is always ideal, preferably done at each individual level.[12, 22-23] Although this can be achieved by wearing an electronic watch, its application in mass screening is limited by its high cost. As an alternative, thermal sensitive materials can be used as a cheap qualitative thermometer for fever screening, but its accuracy is constrained by its wide transition temperature window.[24-29]

Herein, we present a simple method to prepare a highly thermosensitive hydrogel with a narrow transition temperature window for real-time fever alert monitoring. The hydrogel is composed of

thermoresponsive poly(N-isopropylacrylamide)-*co*-acrylamide (P(NIPAM-*co*-AM)) microgel embedded in agarose hydrogel (agarose@P(NIPAM-*co*-AM)) and it is capable of turning from transparent to opaque white when its temperature is higher than its cloud point (denoted as color-transition temperature hereinafter). The hydrogel shows a narrow color-transition temperature window: its transmittance decreases from ~70.5% to 17.5% when the temperature increases from 37.2°C to 37.4°C. The large transmittance change of the hydrogel is clearly visible to naked eyes, making it a convenient fever detector. As a matter of fact, the color-transition temperature of the hydrogel can be precisely tuned by simply modulating the ratio of NIPAM comonomer to acrylamide (AM) comonomer during the synthesis, which allows the temperature alert threshold of the hydrogel to be tailored for monitoring other diseases like hyperthermia and hyperpyrexia.

As a proof-of-concept, the agarose@P(NIPAM-*co*-AM) hydrogel with precisely turned color-transition temperature to the threshold of human fever is assembled into a wristband. When the wrist temperature is higher than the color-transition temperature of the hydrogel, the wristband in real time shows a clear color change, alerting an elevated body temperature and calling for immediate medical attention (Figure 1). The designed wristband is cheap and effective and can be massively distributed for mass fever screening especially at those highly congregated places with regular occupants, such as office buildings, schools, university campuses, and even hospitals. It has a great potential to make a solid contribution to inhibit the transmission of COVID-19 during the ongoing pandemic.

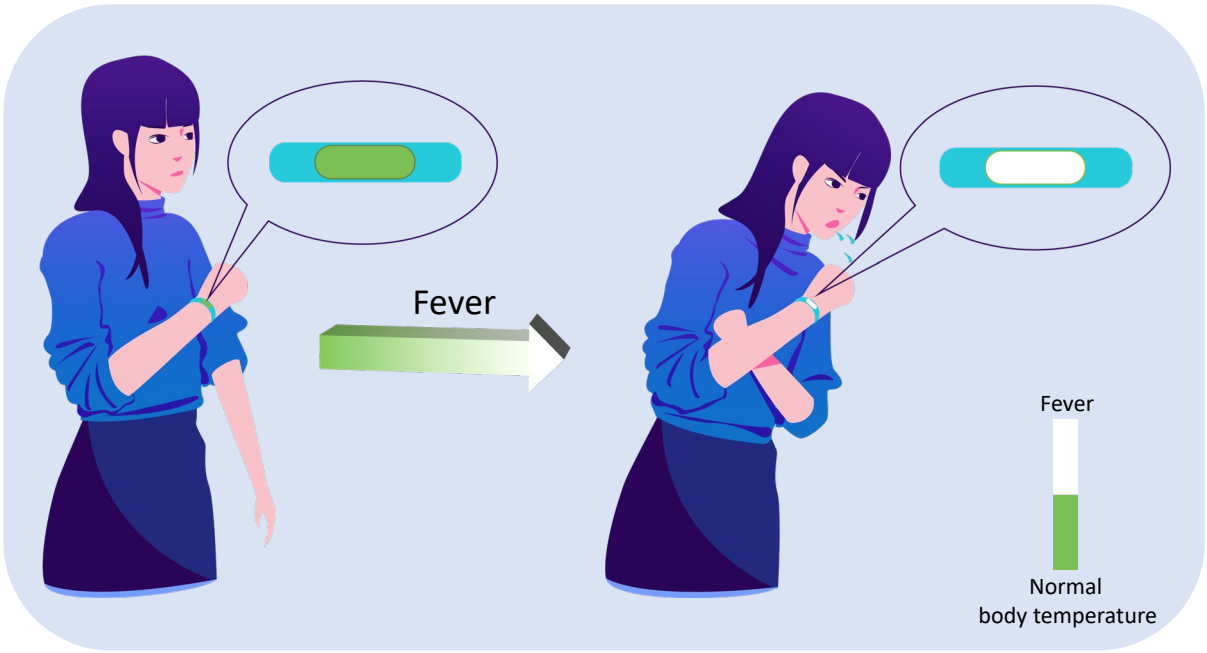

Figure 1. Conceptual illustration of the wristband for real-time personal fever alert. The wristband changes from green to opaque white color when one gets a fever.

Results

The wristband consists of a silicone rubber band as a holder and a hydrogel-based detector where the agarose@P(NIPAM-co-AM) hydrogel is placed on top of a thin aluminum sheet and then encapsulated by a polymethylmethacrylate (PMMA) enclosure, as shown in Figure S1. The microgel of P(NIPAM-co-AM) is embedded inside the matrix of agarose and endows the composite hydrogel with temperature responsibility.

To enhance the visual readability of the detector, the surface of the aluminum sheet is dyed green. As a result, the detector appears green under normal wrist temperature because the hydrogel is transparent in this condition, and it turns opaque white when the wrist temperature is higher than a fever temperature.

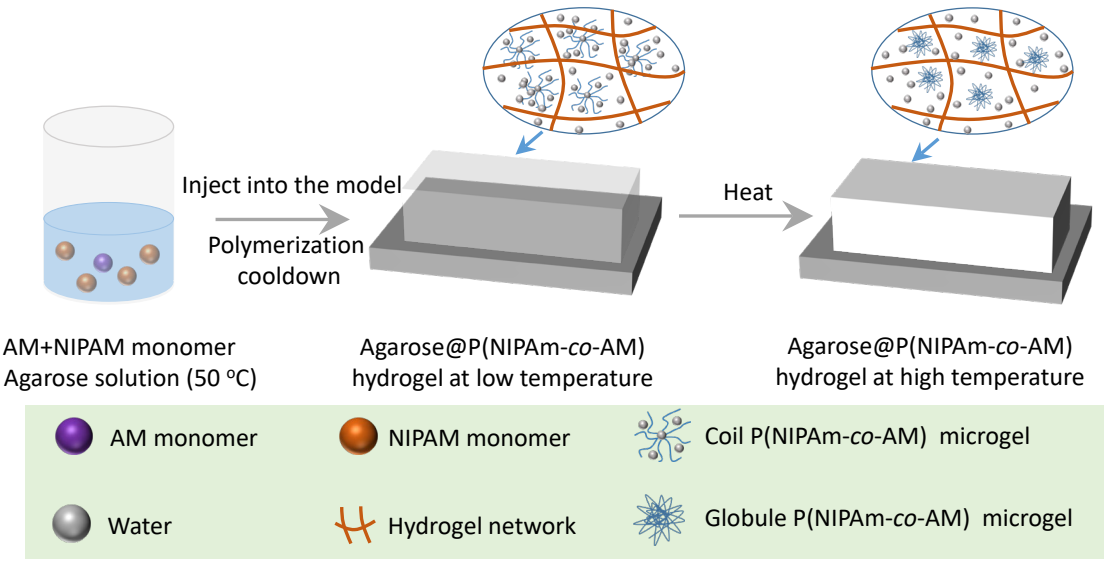

Figure 2 schematic illustration of the agarose@P(NIPAM-co-AM) preparation process.

Preparation of Agarose@P(NIPAM-*co*-AM) Hydrogel. The P(NIPAM-co-AM) copolymer microgel is composed of a main polymer chain of PNIPAM and AM comonomer. PNIPAM is a well-known thermo-responsive polymer with a lower critical transition temperature (LCST) or cloud point (T_{cp}) of around 32°C and it has a structure containing a hydrophobic backbone and a hydrophilic amide group capped by a hydrophobic iso-propyl moiety (Figure S2.)[30-32]. Below its T_{cp}, PNIPAM chains remain in a coil conformation due to the hydrogen bonding of hydrophilic amide groups with surrounding water molecules, exhibiting a soluble and transparent look. Above its T_{cp}, the hydrophobic interactions between the hydrophobic backbone and isopropyl groups become dominant, leading to the intra or intermolecular aggregation of hydrophobic moieties. Consequently, PNIPAM chains collapse into a globule at molecular level, resulting in a macroscopically opaque solution.

In theory, increasing the polymer-water interaction results in an elevated T_{cp} while an enhanced polymer-polymer interactions leads to a lower T_{cp}.[33-36] Since the inherent T_{cp} of PNIPAM is lower than body temperature (~37°C), acrylamide (AM) monomers is introduced into PNIPAM, forming

a copolymer to enhance its T_{cp}.[32, 37] It is expected that the T_{cp} of PNIPAM chain can be precisely tuned by incorporating the hydrophilic amide group of AM.

The reversible transition of PNIPAM in response to temperature necessitates co-presence of water in its structure. In this work, the P(NIPAM-co-AM) microgel, instead of its bulk hydrogel, is synthesized as the former overcomes the drawback of volumetric shrinkage and irreversible dehydration of the latter during transition.[24-26] To immobilize the microgel, agarose hydrogel is chosen as a supporting matrix owing to its stability, transparency, low cost, easy synthesis and biocompatibility.[38] As a matter of fact, agarose is a common food additive.[39]

The agarose@P(NIPAM-co-AM) hydrogel is prepared by a simple 1-step method, as shown in Figure 2. The precursor solution is obtained by dissolving into water the reactants, including agarose, NIPAM monomer and AM monomer, catalyst, initiator, to form a clear and homogeneous mixture and the hydrogel is obtained after the simultaneous polymerization and gelation for 12 h at room temperature. Before complete gelation, the precursor solution is transferred into a customized mold with a desired shape. When the temperature is elevated to be higher than the T_{cp} of PNIPAM, a distinguishable color change can be observed at the composite hydrogel as it turns from transparent to opaque white. Control experiments are conducted with pure agarose hydrogel and P(NIPAM-co-AM) microgel to confirm the advantage of having agarose hydrogel to host the microgel, whose details can be found in supporting information (Figure S3 and Note S1).

SEM image of the agarose@P(NIPAM-co-AM) hydrogel after freeze-drying shows an irregular porous structure (Figure S4), similar to that of agarose hydrogel. This comparison indicates that the polymerization process of the copolymer has no effect on the pore structure of the agarose hydrogel. Moreover, the P(NIPAM-co-AM) microgel particles can be observed on the walls of the hydrogel with an irregular shape (Figure S4c).

The chemical composition of the agarose@P(NIPAM-co-AM) hydrogel was analyzed by Fourier transform infrared (FTIR) spectra (Figure S5a). In the agarose hydrogel, the broad peaks at ~3420 and ~2910 cm^{-1} can be attributed to stretching vibration of O-H groups and C-H groups, respectively[40]. Furthermore, the bands at ~1156 and ~1072 cm^{-1} are assigned to C-O-C and C-OH stretching vibrations, which are characteristic to agarose[41-42]. For the agarose@P(NIPAM-co-AM), the band at 1547 cm^{-1} corresponds to N-H bending vibration while the band at 1462 cm^{-1} is attributed to the C-N stretching in C-NH_2 of PAM[43-44]. The deformation vibration peaks at ~1388 and ~1368 cm^{-1} are attributed to the C-H bond in isopropyl group of PNIPAM[24, 45], altogether confirming the formation of the P(NIPAM-co-AM) copolymer. X-ray photoemission spectroscopy (XPS) was further used whose results are presented in Figure S5b, c. Compared to the O 1s spectrum of the pure agarose, the peak at ~532.0 eV is ascribed to the C-O-C/C-O-OH units of the agarose and the new peak at ~531.9 eV is attributed to the O=C-N unit in the amid group of PNIPAM or PAM[46-47], further confirming the formation of the PNIPAM and/or PAM moieties in the composite hydrogel.

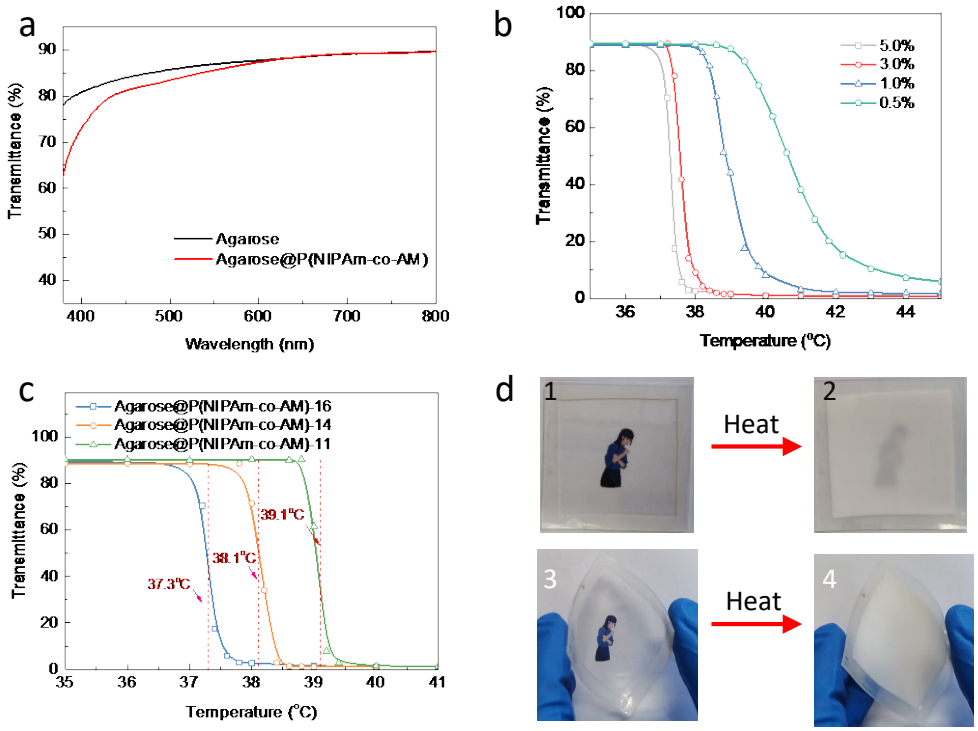

Figure 3. The optical performance of the agarose@P(NIPAM-co-AM) hydrogel. (a) Visible light transmission spectra of the agarose hydrogel and agarose@P(NIPAM-co-AM) hydrogel at room temperature. (b) Transmittance of the agarose@P(NIPAM-co-AM) hydrogel at the wavelength of 550 nm at different concentrations and (c) molar ratio of NIPAM comonomer to AM comonomer. (d) Photographs of the agarose@P(NIPAM-co-AM) hydrogel at room temperature (left) and 40°C (right).

Optical Performance of the Agarose@P(NIPAM-*co*-AM) Hydrogel. The visible light transmittance of the agarose hydrogel and agarose@P(NIPAM-co-AM) hydrogel is shown in Figure 3a. The transmittance of agarose hydrogel gradually increases from 78.0% to 87.8% between 380 nm and 600 nm, beyond which only a small increment can be observed, reaching 89.7% at 800 nm. Compared to agarose hydrogel, the agarose@P(NIPAM-co-AM) hydrogel shows a slightly lower transmittance below 600 nm but a comparable transmittance above 600 nm.

The decreased transmittance of the agarose@P(NIPAM-co-AM) hydrogel might be caused by the formation of the P(NIPAM-co-AM) microgel inside the hydrogel.

The thermoresponsive behavior of the agarose@P(NIPAM-co-AM) hydrogel was determined by measuring its temperature-dependent transmittance at the wavelength of 550 nm. The measurement was conducted in a home-made experimental setup as shown in Figure S6. Briefly, the hydrogel precursor solution was firstly injected and sandwiched into a quartz glass mold and, after gelation, the hydrogel part of the mold was placed on the hole of a thermostatic table, which maintained a stable temperature during measurement and at the same time permitted the light of the transmittance meter passing through the hydrogel sample.

To tune the color-transition temperature window, we firstly modulate the concentration of P(NIPAM-co-AM) microgel. As shown in Figure 3b, when the concentration is 0.5%, the agarose@P(NIPAM-co-AM) hydrogel shows a transmittance of ~89.4% below 38.6ºC and a visible transmittance change can be observed from 74.8% to 20.1% at a temperature reduction of 2.0ºC, indicating that the hydrogel possesses a wide color-transition temperature window. When the concentration is increased to 1.0%, 3.0% and 5.0%, the color-transition temperature window (defined when the transmittance reduced by over 50%) decreases to 0.8ºC, 0.4ºC and 0.2ºC respectively. Moreover, the color transition temperature is also reduced from ~40.6ºC to ~37.3ºC when the concentration is increased from 0.5% to 5.0%. These results demonstrate that the color-transition temperature window can be reduced by simply increasing the concentration of the P(NIPAM-co-AM) microgel in the hydrogel and in particular, the color-transition temperature window can be as low as 0.2ºC at a concentration of approximately 5.0%, which is well suited for fever alert monitoring. Therefore, the concentration of the microgel in the hydrogel is kept at about 5.0% in the following experiments.

To further tune the color transition temperature for fever monitoring, we modulated the molar ratio of NIPAM comonomer to AM comonomer and the samples are denoted as agarose@P(NIPAM-co-AM)-xx, with xx being molar ratio of the NIPAM comonomer to AM comonomer. As shown in Figure 3c, agarose@P(NIPAM-co-AM)-16 shows an initial transmittance of ~89.1% below 37ºC, and a sharp decrease can be observed in its transmittance from ~70.5% to 17.5% when its temperature increases from 37.2ºC to 37.4ºC. Further increase in temperature decreases the light transmittance to ~2.9 %. As known, normal body temperature can vary by a degree or so, between 36.1ºC and 37.2ºC. A fever is typically defined as body temperature above 37.2ºC[48]. In view of this, agarose@P(NIPAM-co-AM)-16 is a suitable candidate as a fever alert monitor. When the molar ratio is decreased to be 14:1, agarose@P(NIPAM-co-AM)-14 exhibits an abrupt transmittance decrease from 71.5% at 38.0ºC to 31.4% at 38.2ºC. The increased color-transition temperature should be attributed to the increase in the AM in the copolymer, which enhances the polymer-water interaction owing to the increased hydrophilic amide group. Hyperthermia is defined as a body temperature higher than 38.0 ºC (this number may vary from country to country) and is a medical emergency requiring immediate treatment to prevent disability or even death[49]. Since the color-transition temperature of the agarose@P(NIPAM-co-AM)-14 resides nicely near ~38ºC, it can be used specifically for hyperthermia screening. Similarly, the color-transition temperature of the agarose@P(NIPAM-co-AM)-11 is around ~39.1ºC. When the temperature increases from 39.0ºC to 39.2ºC, its transmittance decreases from 61.6% to 7.9%. The above results demonstrate that the color-transition temperature of the agarose@P(NIPAM-co-AM) hydrogel can be facilely tuned and the prepared agarose@P(NIPAM-co-AM) hydrogel shows a narrow color-transition temperature

window that matches well with human fever temperature, which is critical to a successful fever screening.

The visual transparency transition of the agarose@P(NIPAM-co-AM) hydrogel (with a thickness of 1mm) in response to temperature change is shown in Figure 3d1-d2. As clearly seen, at room temperature of ~25ºC, the hydrogel is highly transparent and the picture beneath the mold can be observed clearly. Upon heating at 40.0ºC for 5 min, the hydrogel turns opaque white and the underlying picture is nearly invisible.

The high flexibility of hydrogel allows for fabrication of flexible detector which broadens its application perspective. As shown in Figure 3d3-d4, a thin agarose@P(NIPAM-co-AM) hydrogel film was fabricated on a flexible and transparent polyvinyl chloride (PVC) substrate and exhibits expected transparency change in response to heating.

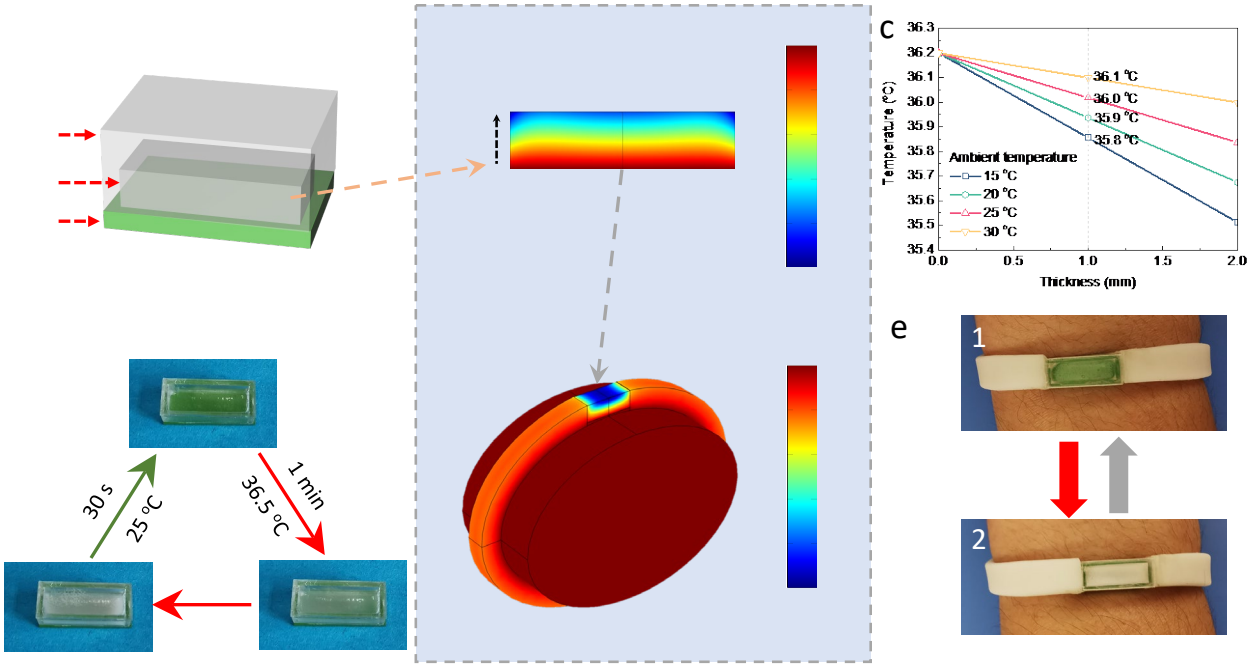

Figure 4. The design and assembly of the wristband for personal fever monitoring. (a) the schematic illustration of the designed fever detector (1. aluminum sheet painted green; 2. hydrogel; 3. PMMA cover); (b) modelled temperature distribution of the wristband (c) and the vertical

temperature profile of the hydrogel in the detector under different ambient temperature; (d) color transition of the detector under different temperatures; (e) the color change of the detector in the wristband at (1) a normal wrist temperature of 35.6ºC and (2) an elevated wrist temperature of 36.7ºC.

The Design and Assembly of the Wristband for fever monitoring. For the purpose of having the agarose@P(NIPAM-co-AM) hydrogel to be used as a sensor to qualitatively screen body fever at individual level, the agarose@P(NIPAM-co-AM) hydrogel was assembled into a wristband to make a wearable and all-in-one device. However, a definite cut-off wrist temperature for fever screening that is internationally agreed upon has not been established. For example, it is recommended that the threshold of wrist temperature for detecting tympanic temperature (>37.2ºC) was 36.2ºC, with a sensitivity of 86.4%.[50] This work adopts this guideline and considers the wrist temperature of >36.2ºC as the threshold temperature for fever. It is worth reemphasizing that the color transition temperature of our hydrogel can be simply modulated to meet the needs of different application scenarios.

The wristband consists of a strap, made by silicone rubber, and a detector, having agarose@P(NIPAM-co-AM) hydrogel as sensing component. As is shown in Figure 4a and Figure S1, the detector is composed of an aluminum sheet with a size of 15x6x1 mm at the bottom, a agarose@P(NIPAM-co-AM) hydrogel layer of 2 mm on the top of the aluminum sheet and a transparent enclosure of PMMA. The aluminum sheet is selected owing to its high thermal conductivity (205 W/m K); the top surface of the aluminum sheet is dyed green by the commercial paint to increase visual contrast during temperature transition. The transparent PMMA enclosure is completely sealed together with the aluminum sheet by UV-curing adhesive. Additionally, an

air gap between the agarose@P(NIPAM-co-AM) hydrogel and the ceiling of PMMA cover is deliberately made to minimize the heat loss caused by thermal conduction and thermal convection.

To make the fever screening more reliable and accurate, the temperature difference between the hydrogel and the wrist need to be considered. A thermal model was first established to simulate the temperature distribution of the hydrogel in the wristband by COMSOL Multiphysics software. With the wrist temperature set at 36.2ºC, the simulated temperature variation along the vertical height of the hydrogel under different ambient temperature is shown in Figure S7. As seen, no significant temperature change can be observed across the aluminum sheet owing to its high thermal conductivity. For the hydrogel, its temperature reduction along vertical direction varies under different ambient temperature, showing a lower decrement at a higher ambient temperature. There is 0.7ºC and 0.2ºC temperature reduction at the ambient temperature of 15ºC and 30ºC respectively (Figure 4c). This should be attributed to the lower temperature difference between the wrist and ambient. On the other hand, the temperature variation across the air gap above the hydrogel is high, exhibiting a decrement by 5.8ºC and 1.7ºC at the ambient temperature of 15ºC and 30ºC respectively. The smaller reduction in the temperature across the hydrogel should be attributed to the low thermal conductivity of the air gap (0.026 W/m K at room temperature), which can be regarded as a thermal insulation.

Since the temperature of the hydrogel is not evenly distributed, the temperature in the middle is used to represent its temperature. For every 5ºC decline in ambient temperature, the temperature disparity between the wrist and hydrogel is decreased by 0.1ºC. As the wristband aims at fever screening in indoor settings, the work designs the wristband to be used at ambient temperature of 25ºC. Under this condition, when the wrist temperature is 36.2ºC, the temperature of the hydrogel is 36.0ºC. The color-transition temperature of the agarose@P(NIPAM-co-AM) hydrogel needs to

be tuned at 36.0°C and thereafter, by modulating the molar ratio of the NIPAM comonomer to AM comonomer, a new agarose @P(NIPAM-co-AM) hydrogel was tailor-made. As shown in Figure S8, the newly prepared agarose@P(NIPAM-co-AM) hydrogel exhibits a sharp reduction in the transmittance from 81.2% at 35.9°C to 31.5% at 36.1°C, confirming that the hydrogel is successfully tuned to the desired color-transition temperature.

The assembled detector is shown in Figure 4d and Figure S9 and owing to the highly transparency of the hydrogel, it appears green and, when the detector was placed on a thermostatic table with the temperature of 36.5°C, it turned to translucent at the end of the first minute and became completely opaque white after further heating for another 1 minute. By cooling at room temperature for only 30 s, the detector recovered to its original green color (the color-transition process can be also found in Supplementary Video 1). The result indicates that the detector possesses a reversible and fast response to small temperature change.

The detector was then assembled with the silicone rubber band and tested on the wrist of a volunteer, as shown in Figure S1 and Figure 4e. It needs to point out firstly that due to the strict safety regulation during COVID-19 pandemic, this project was not permitted any access to any fever patients. Instead, the fever state of the volunteer was simulated by intense indoor exercise. Many previous reports have demonstrated that intense exercise is capable of elevating body temperature to a state similar to a fever[51-52]. Additionally, the measurement at the same person in different states allows for a better consistency and comparability. Firstly, the healthy volunteer wore the wristband for one day and the real wrist temperature of the volunteer was measured by IR camera. A typical picture of the wristband at normal temperature is shown in Figure 4e1. The detector stayed in green during the test and the wrist temperature was measured to be below 36.0°C. Then, after intense indoor exercise for 60 minutes, the wrist temperature was increased to 36.5°C,

which is higher than the threshold of the wrist measurement for a fever as discussed earlier. This confirms the successfully simulated fever state by the intense exercise. At the meanwhile, the detector of the wristband turned into completely opaque white, clearly indicating a fever state. The color transition of the detector agrees well with the result of the infrared thermometer, successfully demonstrating that the designed wristband is capable of being used for real-time fever monitoring. Considering the effect of the sweat, we immersed the wristband in a simulated sweat solution (NaCl: 0.04 M, KCl: 0.005 M, CaCl: 0.375 mM, MgCl: 0.054 mM) for one day and then measured color-transition temperature window of the hydrogel. As shown in Figure S9, the hydrogel exhibited a comparable color-transition temperature window before and after sweat immersion. These results demonstrate that the sweat had little effect on the sensitivity of the wristband.

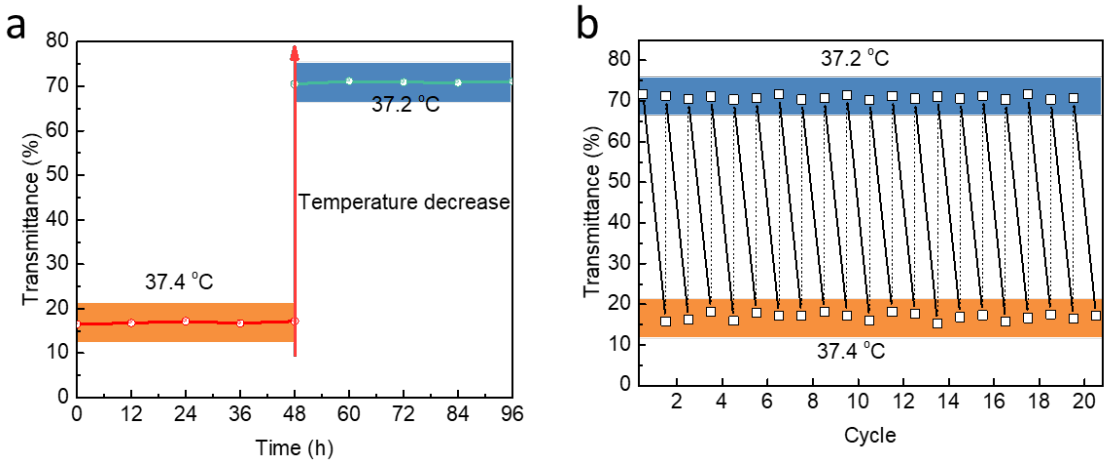

Figure 5. Performance stability evaluation of the agarose@P(NIPAM-*co*-AM) hydrogel. (a) long-term stability and (b) cycle performance.

In order to verify the performance stability of the agarose@P(NIPAM-co-AM)-16 hydrogel for long-time operation, we firstly performed a long-term stability test. The temperature of the hydrogel was elevated to a high temperature (37.4°C) and lasted for 2 days, then cooled to a lower temperature (37.2°C) and lasted for another 2 days. As shown in Figure 5a, when the hydrogel was kept at 37.4°C, it exhibited a stable transmittance of below ~18% during the 2-days test and when

the temperature was reduced to 37.2ºC, the transmittance was increased back to ~71.0%, indicating that the hydrogel possesses an excellent long-term durability. In addition, we further investigated cycle performance of the hydrogel by 20 heating/cooling cycles. At each heating/cooling cycle, the agarose@P(NIPAM-co-AM)-16 hydrogel was heated up to and maintained at 37.4ºC for 1 hour, followed by cooling at room temperature for another 1 hour. As shown in Figure 5b, in the 20 cycles, the transmittance of the hydrogel was at the range of 70.1~72.3% at 37.2ºC while it decreased to the range of 15.8~18.1% at 37.4ºC. These results demonstrate that the color-transition process of the hydrogel is highly reversible and stable.

Discussion.

Although temperature measurements at armpit and in ear give more reliable and accurate temperature readings but they lack convenience. Thus, they can be ruled out as a massive measure for continuous and real-time fever screening during a pandemic. In comparison, mass fever screening based on wrist or forehead temperature is faster and thus more convenient as the defense again the pandemic. However, the wrist measurement falls has a lower sensitivity (e.g. 86.4%[50]) for fever detecting relative to armpit and ear measurement, and it can be affected by the surrounding temperature. In particular, the measurement by the hydrogel would be invalid when the surrounding temperature is higher than body temperature. Furthermore, the intensive exercise would also affect the accuracy of the measurement as the body temperature can be increased after intensive exercise. While a typical thermometer is capable of detecting different body temperature-related diseases such as fever, hyperthermia and hyperpyrexia, the hydrogel reported in this work can only detect a given temperature change because it can only respond to a temperature set point. These drawbacks may limit its further application.

The agarose@P(NIPAM-co-AM) hydrogel is prepared by a simple one-step method under mild condition and this process is easy to be scaled up for mass production. In addition, the preparation of a detector for one wristband only demands 100 ul of precursor solution, which contains 5.34 mg of NIPAM comonomer, 0.22 mg of AM comonomer, 0.19 mg of potassium persulfate, 0.12 mg of N,N,N',N'-tetramethylethylenediamine and 0.48 mg of agarose (taking agarose@P(NIPAM-co-AM)-16 as an example). Based on the current market prices of these chemicals (Table S1), to synthesize 100 ml of precursor solution for the preparation of ~1000 detectors, the raw material cost is estimated to be only ~2.0 ¥ (0.29 $, the exchange rate was obtained in 03 Sep. 2020), which, in combination with inexpensive rubber band and aluminum sheet, demonstrates that the hydrogel based fever screening is a very cheap and easily affordable approach to help fight infection-induced pandemic, especially ongoing COVID-19. Given its low cost, the wearable fever detector can be made disposal, which can be desirable at hospital and shopping mall settings where many transient visitors frequent. The easily identifiable color change of the detector certainly alarms everyone around a potential fever patient. Since the agarose@P(NIPAM-co-AM) hydrogel shows a good softness[53] and possesses the capabilities to conform to various geometries,[54] it can be also assembled into various wearable devices such as a headband to screen fever based on forehead temperature. The wearable fever detector can be applied inside a family, at workplaces, schools, hospitals, among others for early warming of a potentially virus infected cases and to alert for immediate medical attentions. Moreover, the PNIPAM-based microgel is believed to possess an excellent reversibility and durability[55-56], and the device thus is expected to have a long lifetime (e.g. several years).

For fever detecting, the accuracy of the agarose@P(NIPAM-co-AM) hydrogel is 0.2°C, which is comparable to that of the commercial electrical wearable watch (e.g. Empatica E4 Watch,

Empatica, Milan, Italy), indicating that the hydrogel is capable of reliably detecting a fever. Moreover, the agarose@P(NIPAM-co-AM) hydrogel have a longer continuous working period because it does not battery to power itself, which represents a greener method for fever alert monitoring.

The accuracy of the wristband detector can be affected by the ambient temperature, with every 5°C decrement in ambient temperature resulting in a 0.1°C offset in the hydrogel detector. This can be solved by a better heat insulation method. For example, the hydrogel can be wrapped by a transparent aerogel with a low thermal conductivity to reduce the effect of thermal conduction and thermal convection. Moreover, at a given surrounding temperature, the color-transition temperature window can be tailored to the corresponding threshold temperature by simply modulating the molar ratio of NIPAM comonomer to acrylamide (AM) comonomer during the synthesis. This allows the detector to be used in various situations including outdoor settings.

Moreover, In this work, both P(NIPAM-co-AM) microgel and agarose hydrogel possess good biocompatibility and have been reported as materials in various wearable devices.[57-58] Therefore, the agarose@P(NIPAM-co-AM) hydrogel can be deemed as bio-safe wearable sensor.

Conclusion

In conclusion, we have developed an agarose@P(NIPAM-co-AM) hydrogel-based fever detector for early detection of virus-infected cases. The design and fabrication of the detector in this work provide a new insight into making inexpensive fever detector for real-time and convenient screening of fever cases at mass scale during a pandemic.

Methods

Materials. N-Isopropylacrylamide (NIPAM), acrylamide (AM), potassium persulfate (KPS) and N,N,N',N'-tetramethylethylenediamine (TEMED) were purchased from Sigma Aldrich. The Agarose was purchased from Gene Company LTD. All the chemicals were used as received without further purification.

Fabrication of the Agar@P(NIPAM-*co*-AM) hydrogel. Agarose@P(NIPAM-*co*-AM) hydrogel was prepared by a simple one-step method. Typically, 2.2636 g of NIPAM and 0.0903 g of AM were added into 20 ml of pure water (18 MΩ cm) in a beaker and mixed by a magnetic bar until total dissolution. Then, 2 ml of KPS (4 wt% aqueous solution) was added to the mixture, followed by 50 ul of TEMED. Next, 20 ml of agarose solution (1 wt% aqueous solution, stored at 50^{o}C oven) was added into the mixture solution. Finally, the mixture solution was injected into the glass mold for characterization. Polymerization and gelation were performed simultaneously at room temperature for 12 h. The cloud point of the sample was simply modulated by varying the mole ratio between NIPAM monomer and AM monomer, and the obtained hydrogel was denoted as Agarose@P(NIPAM-*co*-AM)-x (x represents that the mole ratio between NIPAM and AM).

Transparency at different temperature test: The transparency of the samples as a function of temperature was measured by a home-made set-up, as shown in Figure S6. The sample for the measurement was prepared by injecting the precursor solution into quartz glass mold and after gelation, it was placed on top of the hole of a thermostatic table (DB-H, Hongze Technology). The hole of the thermostatic table was located under the light source of the transmittance meter (LS108A), allowing the light passing through the sample. Moreover, the temperature of the sample was further calibrated by a FLUKE Ti450 IR camera.

Color-transition test of the wristband. The wristband was firstly put on the wrist of a normal volunteer (the consent letter can be found at the last page) and the wrist temperature was then

measured by an infrared thermometer (Yuwell). The fever state of the volunteer was simulated by one-hour indoor intensive exercise (running and press-up) and the wrist temperature was measured by the same infrared thermometer consistently throughout the experiments.

Characterization. The SEM images were obtained on a FEI field emission scanning electron microscope (Verios G4). The FITR spectra was obtained from a Bruker TENSOR 27 FTIR spectrometer. XPS spectra was obtained from a Kratos AXIS Ultra DLD XPS spectrometer. The UV-VIS spectra was obtained on a Tecan Infinite M200 PRO.

ASSOCIATE CONTENT

Supporting Information

The Supporting Information is available free of charge at XXXX

Additional note and figures, including structure of wristband, PNIPAM chemical formulas, SEM images, FTIR

AUTHOR INFORMATION

Corresponding Author:

E-mail: zhanghepeng@nwpu.edu.cn (H. Zhang), peng.wang@kaust.edu.sa (P. Wang)

Authors

Wenbin Wang- Water Desalination and Reuse Center, King Abdullah University of Science and Technology, Thuwal 23955-6900, Saudi Arabia.

Chen Wu- Key Laboratory of Special Functional and Smart Polymer Materials of Ministry of Industry and Information Technology, School of Chemistry and Chemical Engineering, Northwestern Polytechnical University, Xi'an, 710129, PR China.

Kai Zhu- Key Laboratory of Special Functional and Smart Polymer Materials of Ministry of Industry and Information Technology, School of Chemistry and Chemical Engineering, Northwestern Polytechnical University, Xi'an, 710129, PR China.

Fang Chen- Key Laboratory of Special Functional and Smart Polymer Materials of Ministry of Industry and Information Technology, School of Chemistry and Chemical Engineering, Northwestern Polytechnical University, Xi'an, 710129, PR China.

Jingjing Zhou- Key Laboratory of Special Functional and Smart Polymer Materials of Ministry of Industry and Information Technology, School of Chemistry and Chemical Engineering, Northwestern Polytechnical University, Xi'an, 710129, PR China.

Yusuf Shi- Water Desalination and Reuse Center, King Abdullah University of Science and Technology, Thuwal 23955-6900, Saudi Arabia.

Chenlin Zhang- Water Desalination and Reuse Center, King Abdullah University of Science and Technology, Thuwal 23955-6900, Saudi Arabia.

Renyuan Li- Water Desalination and Reuse Center, King Abdullah University of Science and Technology, Thuwal 23955-6900, Saudi Arabia.

Mengchun Wu- Water Desalination and Reuse Center, King Abdullah University of Science and Technology, Thuwal 23955-6900, Saudi Arabia.

Sifei Zhuo- Key Laboratory of Special Functional and Smart Polymer Materials of Ministry of Industry and Information Technology, School of Chemistry and Chemical Engineering, Northwestern Polytechnical University, Xi'an, 710129, PR China.

Author contribution

W.W. and P.W. proposed the idea. W.W., H.Z. and P.W. designed the experiments. W.W. conducted the experiments. C.W., K.Z., and F.C. helped in the SEM measurement and FTIR

measurement. C.Z. and R.L. helped draw the schematics. Y.S., H.Z., W.W., M.W., C.Z., S.Z., H.Z., C.W. and P.W. all contributed to writing and revising the paper.

Acknowledgements

The authors are grateful to the KAUST for very generous financial support.

Notes

P.W. and W.W. have pending patent application based on the results of this work.

REFERENCE

(1) Chiu, W.; Lin, P.; Chiou, H.; Lee, W.; Lee, C.; Yang, Y.; Lee, H.; Hsieh, M.; Hu, C.; Ho, Y. Infrared Thermography to Mass-Screen Suspected SARS Patients with Fever. *Asia Pac. J. Public Health* **2005,** *17* (1), 26-28.
(2) Muller, M.; Richardson, S.; McGeer, A.; Dresser, L.; Raboud, J.; Mazzulli, T.; Loeb, M.; Louie, M. Early Diagnosis of SARS: Lessons from the Toronto SARS Outbreak. *Eur. J. Clin. Microbiol.* **2006,** *25* (4), 230-237.
(3) Deng, J.-F.; Olowokure, B.; Kaydos-Daniels, S.; Chang, H.-J.; Barwick, R.; Lee, M.-L.; Deng, C.-Y.; Factor, S.; Chiang, C.-E.; Maloney, S. Severe Acute Respiratory Syndrome (SARS): Knowledge, Attitudes, Practices and Sources of Information among Physicians Answering a SARS Fever Hotline Service. *Public Health* **2006,** *120* (1), 15-19.
(4) Zhang, J.; Zhou, L.; Yang, Y.; Peng, W.; Wang, W.; Chen, X. Therapeutic and Triage Strategies for 2019 Novel Coronavirus Disease in Fever Clinics. *Lancet Respir. Med.* **2020,** *8* (3), e11-e12.
(5) Chen, J.; Qi, T.; Liu, L.; Ling, Y.; Qian, Z.; Li, T.; Li, F.; Xu, Q.; Zhang, Y.; Xu, S. Clinical Progression of Patients with COVID-19 in Shanghai, China. *J. Hosp. Infect.* **2020,** *80* (5), e1-e6.
(6) Lorenz, C.; Azevedo, T. S.; Chiaravalloti-Neto, F. COVID-19 and Dengue Fever: A Dangerous Combination for the Health System in Brazil. *Travel Med. Infect Dis.* **2020**, 101659.
(7) Olson, D. R.; Heffernan, R. T.; Paladini, M.; Konty, K.; Weiss, D.; Mostashari, F. Monitoring the Impact of Influenza by Age: Emergency Department Fever and Respiratory Complaint Surveillance in New York City. *PLos. Med.* **2007,** *4* (8), e247.
(8) Peiris, M.; Yuen, K.; Leung, C.; Chan, K.; Ip, P.; Lai, R.; Orr, W.; Shortridge, K. Human Infection with Influenza H9N2. *Lancet.* **1999,** *354* (9182), 916-917.
(9) Evenson, D. P.; Jost, L. K.; Corzett, M.; Balhorn, R. Characteristics of Human Sperm Chromatin Structure Following an Episode of Influenza and High Fever: A Case Study. *J. Androl.* **2000,** *21* (5), 739-746.
(10) Evans, S. S.; Repasky, E. A.; Fisher, D. T. Fever and the Thermal Regulation of Immunity: The Immune System Feels the Heat. *Nat. Rev. Immunol.* **2015,** *15* (6), 335-349.
(11) Ng, E. Y.; Kaw, G. J.; Chang, W. M. Analysis of IR Thermal Imager for Mass Blind Fever Screening. *Microvasc. Res.* **2004,** *68* (2), 104-9, DOI: 10.1016/j.mvr.2004.05.003.
(12) Holt, S. G.; Yo, J. H.; Karschimkus, C.; Volpato, F.; Christov, S.; Smith, E. R.; Hewitson, T. D.; Worth, L. J.; Champion De Crespigny, P. Monitoring Skin Temperature at the Wrist in Hospitalised Patients May Assist in the Detection of Infection. *Intern. Med. J.* **2020,** *50* (6), 685-690, DOI: 10.1111/imj.14748.
(13) Chen, H. Y.; Chen, A.; Chen, C. Investigation of the Impact of Infrared Sensors on Core Body Temperature Monitoring by Comparing Measurement Sites. *Sensors (Basel)* **2020,** *20* (10), 2885, DOI: 10.3390/s20102885.
(14) Niven, D. J.; Gaudet, J. E.; Laupland, K. B.; Mrklas, K. J.; Roberts, D. J.; Stelfox, H. T. Accuracy of Peripheral Thermometers for Estimating Temperature: A Systematic Review and Meta-Analysis. *Ann. Intern. Med.* **2015,** *163* (10), 768-777.
(15) Nishiura, H.; Kamiya, K. Fever Screening During the Influenza (H1N1-2009) Pandemic at Narita International Airport, Japan. *BMC Infect. Dis.* **2011,** *11* (1), 111.
(16) Tay, J.; Ng, Y. F.; Cutter, J.; James, L. Influenza a (H1N1-2009) Pandemic in Singapore—Public Health Control Measures Implemented and Lessons Learnt. *Ann. Acad. Med. Singap.* **2010,** *39* (4), 313.

(17) Hewlett, A. L.; Kalil, A. C.; Strum, R. A.; Zeger, W. G.; Smith, P. W. Evaluation of an Infrared Thermal Detection System for Fever Recognition During the H1N1 Influenza Pandemic. *Infect. Control Hosp. Epidemiol.* **2011,** *32* (5), 504-506.
(18) Lee, V. J.; Chiew, C. J.; Khong, W. X. Interrupting Transmission of COVID-19: Lessons from Containment Efforts in Singapore. *J. Travel Med.* **2020,** *27* (3), taaa039.
(19) Viner, R. M.; Russell, S. J.; Croker, H.; Packer, J.; Ward, J.; Stansfield, C.; Mytton, O.; Bonell, C.; Booy, R. School Closure and Management Practices During Coronavirus Outbreaks Including COVID-19: A Rapid Systematic Review. *Lancet Child Adolesc. Health.* **2020,** *4* (5), 397-404.
(20) Tan, L. Preventing the Transmission of COVID-19 Amongst Healthcare Workers. *J. Hosp. Infect.* **2020,** *105* (2), 364-365.
(21) Jeong, H.; Rogers, J. A.; Xu, S. Continuous on-Body Sensing for the COVID-19 Pandemic: Gaps and Opportunities. *Science Advances* **2020,** *6* (36), eabd4794.
(22) Lou, D.; Pang, Q.; Pei, X.; Dong, S.; Li, S.; Tan, W.-q.; Ma, L. Flexible Wound Healing System for Pro-Regeneration, Temperature Monitoring and Infection Early Warning. *Biosens. Bioelectron.* **2020,** *162*, 112275.
(23) Hsiao, S.-H.; Chen, T.-C.; Chien, H.-C.; Yang, C.-J.; Chen, Y.-H. Measurement of Body Temperature to Prevent Pandemic COVID-19 in Hospitals in Taiwan: Repeated Measurement Is Necessary. *J. Hosp. Infect.* **2020,** *105* (2), 360-361.
(24) Wu, M.; Shi, Y.; Li, R.; Wang, P. Spectrally Selective Smart Window with High near-Infrared Light Shielding and Controllable Visible Light Transmittance. *ACS Appl. Mater. Interfaces* **2018,** *10* (46), 39819-39827.
(25) Haq, M. A.; Su, Y.; Wang, D. Mechanical Properties of PNIPAM Based Hydrogels: A Review. *Mater. Sci. Eng. C* **2017,** *70*, 842-855.
(26) Cao-Luu, N.-H.; Pham, Q.-T.; Yao, Z.-H.; Wang, F.-M.; Chern, C.-S. Synthesis and Characterization of PNIPAM Microgel Core–Silica Shell Particles. *J. Mater. Sci.* **2019,** *54* (10), 7503-7516.
(27) Guo, Y.; Bae, J.; Fang, Z.; Li, P.; Zhao, F.; Yu, G. Hydrogels and Hydrogel-Derived Materials for Energy and Water Sustainability. *Chemical Reviews* **2020,** *120* (15), 7642-7707.
(28) Zhou, X.; Zhang, P.; Zhao, F.; Yu, G. Super Moisture Absorbent Gels for Sustainable Agriculture Via Atmospheric Water Irrigation. *ACS Materials Letters* **2020,** *2* (11), 1419-1422.
(29) Zhou, X.; Lu, H.; Zhao, F.; Yu, G. Atmospheric Water Harvesting: A Review of Material and Structural Designs. *ACS Materials Letters* **2020,** *2* (7), 671–684.
(30) Halperin, A.; Kroger, M.; Winnik, F. M. Poly(N-Isopropylacrylamide) Phase Diagrams: Fifty Years of Research. *Angew. Chem. Int. Ed.* **2015,** *54* (51), 15342-67, DOI: 10.1002/anie.201506663.
(31) Heskins, M.; Guillet, J. E. Solution Properties of Poly (N-Isopropylacrylamide). *J. Macromol. Sci. A.* **1968,** *2* (8), 1441-1455.
(32) de Oliveira, T. E.; Mukherji, D.; Kremer, K.; Netz, P. A. Effects of Stereochemistry and Copolymerization on the LCST of PNIPAm. *J. Chem. Phys.* **2017,** *146* (3), 034904, DOI: 10.1063/1.4974165.
(33) Xia, Y.; Burke, N. A.; Stöver, H. D. End Group Effect on the Thermal Response of Narrow-Disperse Poly (N-Isopropylacrylamide) Prepared by Atom Transfer Radical Polymerization. *Macromolecules* **2006,** *39* (6), 2275-2283.
(34) Pamies, R.; Zhu, K.; Kjøniksen, A.-L.; Nyström, B. Thermal Response of Low Molecular Weight Poly-(N-Isopropylacrylamide) Polymers in Aqueous Solution. *Polym. Bull.* **2008,** *62* (4), 487-502, DOI: 10.1007/s00289-008-0029-4.

(35) Wei, G.; Yang, D.; Zhang, T.; Yue, X.; Qiu, F. Thermal-Responsive PNIPAm-Acrylic/Ag NRs Hybrid Hydrogel with Atmospheric Window Full-Wavelength Thermal Management for Smart Windows. *Sol. Energy Mater. Sol.* **2020,** *206*, 110336, DOI: 10.1016/j.solmat.2019.110336.
(36) Jain, K.; Vedarajan, R.; Watanabe, M.; Ishikiriyama, M.; Matsumi, N. Tunable LCST Behavior of Poly(N-Isopropylacrylamide/Ionic Liquid) Copolymers. *Polym. Chem.* **2015,** *6* (38), 6819-6825, DOI: 10.1039/c5py00998g.
(37) Dalkas, G.; Pagonis, K.; Bokias, G. Control of the Lower Critical Solution Temperature—Type Cononsolvency Properties of Poly(N-Isopropylacrylamide) in Water—Dioxane Mixtures through Copolymerisation with Acrylamide. *Polymer* **2006,** *47* (1), 243-248, DOI: 10.1016/j.polymer.2005.10.115.
(38) Tanaka, T.; Urabe, Y.; Nishide, D.; Kataura, H. Continuous Separation of Metallic and Semiconducting Carbon Nanotubes Using Agarose Gel. *Appl. Phys. Express* **2009,** *2* (12), 125002.
(39) Pokusaeva, B. G.; Karlova, S. P.; Nekrasova, D. A.; Zakharova, N. S.; Khramtsova, D. P.; Reznika, V. V.; Vyazminb, A. V.; Shumovab, N. V. Agarose Gels with Bioresorbable Additives: The Kinetics of the Formation, Structure, Some Properties. *Chem. Eng.* **2019,** *74*, 34.
(40) Singh, R.; Singh, A. Synthesis, Characterization and Rheological Properties of Guaran Grafted Polyacrylamide (gg-PAM) Copolymer. *Int. J. Appl. Biol. Pharm.* **2010,** *1*, 897-902.
(41) Mouanda, B.; Eyeffa, V.; Palacin, S. Agarose-Based Hydrogel as an Electrografting Cell. *J. Appl. Electrochem.* **2008,** *39* (3), 313-320, DOI: 10.1007/s10800-008-9675-3.
(42) Guerrero, P.; Etxabide, A.; Leceta, I.; Penalba, M.; de la Caba, K. Extraction of Agar from Gelidium Sesquipedale (Rhodopyta) and Surface Characterization of Agar Based Films. *Carbohydr. Polym.* **2014,** *99*, 491-8, DOI: 10.1016/j.carbpol.2013.08.049.
(43) Li, C.; Xue, F.; Ding, E. Preparation of Polyacrylamide Grafted Collagen Extracted from Leather Wastes and Their Application in Kaolin Flocculation. *J. Appl. Polym. Sci.* **2015,** *132* (13), n/a-n/a, DOI: 10.1002/app.41556.
(44) Shi, Y.; Ma, C.; Peng, L.; Yu, G. Conductive "Smart" Hybrid Hydrogels with PNIPAM and Nanostructured Conductive Polymers. *Adv. Funct. Mater.* **2015,** *25* (8), 1219-1225, DOI: 10.1002/adfm.201404247.
(45) Futscher, M. H.; Philipp, M.; Müller-Buschbaum, P.; Schulte, A. The Role of Backbone Hydration of Poly (N-Isopropyl Acrylamide) across the Volume Phase Transition Compared to Its Monomer. *Sci. Rep.* **2017,** *7* (1), 1-10.
(46) Luo, F.; Chen, Z.; Megharaj, M.; Naidu, R. Simultaneous Removal of Trichloroethylene and Hexavalent Chromium by Green Synthesized Agarose-Fe Nanoparticles Hydrogel. *Chem. Eng. J.* **2016,** *294*, 290-297, DOI: 10.1016/j.cej.2016.03.005.
(47) Shih, C.-M.; Wu, Y.-L.; Wang, Y.-C.; Kumar, S. R.; Tung, Y.-L.; Yang, C.-C.; Lue, S. J. Ionic Transport and Interfacial Interaction of Iodide/Iodine Redox Mechanism in Agarose Electrolyte Containing Colloidal Titanium Dioxide Nanoparticles. *J. Photochem. Photobiol. A* **2018,** *356*, 565-572, DOI: 10.1016/j.jphotochem.2018.01.034.
(48) Jameson, J. L. *Harrison's Principles of Internal Medicine*, McGraw-Hill Education: 2018.
(49) Axelrod, Y. K.; Diringer, M. N. Temperature Management in Acute Neurologic Disorders. *Neurologic clinics* **2008,** *26* (2), 585-603.
(50) Chen, G.; Xie, J.; Dai, G.; Zheng, P.; Hu, X.; Lu, H.; Xu, L.; Chen, X.; Chen, X. Validity of Wrist and Forehead Temperature in Temperature Screening in the General Population During the Outbreak of 2019 Novel Coronavirus: A Prospective Real-World Study. *medRxiv* **2020**.

(51) Deschamps, A.; Levy, R.; Cosio, M.; Marliss, E.; Magder, S. Effect of Saline Infusion on Body Temperature and Endurance During Heavy Exercise. *J. Appl. Physiol.* **1989,** *66* (6), 2799-2804.
(52) Saltin, B.; Hermansen, L. Esophageal, Rectal, and Muscle Temperature During Exercise. *J. Appl. Physiol.* **1966,** *21* (6), 1757-1762.
(53) Du, X.; Cui, H.; Xu, T.; Huang, C.; Wang, Y.; Zhao, Q.; Xu, Y.; Wu, X. Reconfiguration, Camouflage, and Color‐Shifting for Bioinspired Adaptive Hydrogel‐Based Millirobots. *Advanced Functional Materials* **2020,** *30* (10), 1909202.
(54) Zhao, Q.; Li, C.; Shum, H. C.; Du, X. Shape-Adaptable Biodevices for Wearable and Implantable Applications. *Lab on a Chip* **2020,** *20*, 4321-4341.
(55) Zhao, F.; Zhou, X.; Liu, Y.; Shi, Y.; Dai, Y.; Yu, G. Super Moisture‐Absorbent Gels for All‐Weather Atmospheric Water Harvesting. *Advanced Materials* **2019,** *31* (10), 1806446.
(56) Tian, J.; Peng, H.; Du, X.; Wang, H.; Cheng, X.; Du, Z. Hybrid Thermochromic Microgels Based on Ucnps/PNIPAm Hydrogel for Smart Window with Enhanced Solar Modulation. *Journal of Alloys and Compounds* **2020**, 157725.
(57) Amjadi, M.; Sheykhansari, S.; Nelson, B. J.; Sitti, M. Recent Advances in Wearable Transdermal Delivery Systems. *Advanced Materials* **2018,** *30* (7), 1704530.
(58) Su, X.; Borayek, R.; Li, X.; Herng, T. S.; Tian, D.; Lim, G. J. H.; Wang, Y.; Wu, J.; Ding, J. Integrated Wearable Sensors with Bending/Stretching Selectivity and Extremely Enhanced Sensitivity Derived from Agarose-Based Ionic Conductor and Its 3d-Shaping. *Chemical Engineering Journal* **2020,** *389*, 124503.

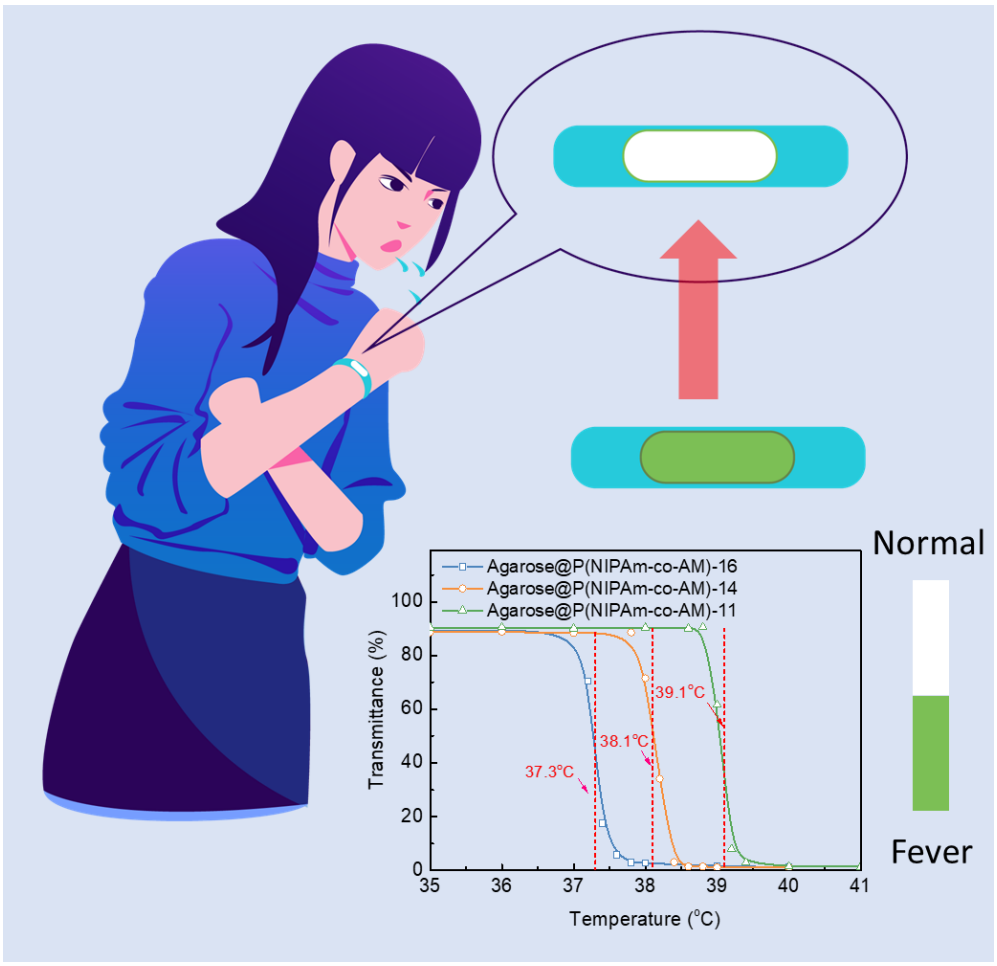

Table of Contents